CONF-841184--24

NEUTRON SCATTERING INVESTIGATION OF MAGNETIC EXCITATIONS AT HIGH ENERGY TRANSFERS (invited)

CONF-841184--24
DE85 004069

C.-K. Loong

Intense Pulsed Neutron Source Program

Argonne National Laboratory, Argonne, IL 60439

With the advance of pulsed spallation neutron sources, neutron scattering investigation of elementary excitations in magnetic materials can now be extended to energies up to several hundreds of meV. We have measured, using chopper spectrometers and time-of-flight techniques, the magnetic response functions of a series of d and f transition metals and compounds over a wide range of energy and momentum transfer. In PrO_2, UO_2, $BaPrO_3$ and CeB_6 we observed crystal-field transitions between the magnetic ground state and the excited levels in the energy range from 40 to 260 meV. In materials exhibiting spin-fluctuation or mixed-valent character such as $Ce_{.74}Th_{.26}$, on the other hand, no sharp crystal-field lines but a broadened quasielastic magnetic peak was observed. The line width of the quasielastic component is thought to be connected to the spin-fluctuation energy of the 4f electrons. The significance of the neutron scattering results in relation to the ground state level structure of the magnetic ions and the spin-dynamics of the f electrons is discussed. Recently, in a study of the spin-wave excitations in itinerant magnetic systems, we have extended the spin-wave measurements in ferromagnetic iron up to about 160 meV. Neutron scattering data at high energy transfers are of particular interest because they provide direct comparison with recent theories of itinerant magnetism.

PACS Numbers: 28.20, 75.30, 75.50

I. Introduction

Information on the properties of the ground state electronic wave function and the associated elementary excitations is of fundamental importance in magnetism. For the "normal" rare-earth compounds and alloys in which the interaction between the 4f ions is weak, the ground state of the rare-earth ions given by Hund's Rule is split by the crystal field. The splittings within the ground state multiplet vary from a few meV for metallic systems to hundreds of meV for ionic insulators. The separations between different J-multiplets are usually of larger energies. In the case of rare-earth mixed-valent materials, on the other hand, it is believed that the spin-fluctuation energy of the 4f electrons is comparable or larger than the crystal-field splitting. As a result, no sharp crystal-field lines but a broad quasielastic feature is observed in the excitation spectrum. The line widths of the quasielastic component may extend to energies above 100 meV. Measurements of the widths of the excitation spectra, in principle, can provide a measure of the lifetime of the 4f electrons in the ground state of the system.

While in general the Russell-Saunders coupling scheme works quite well in the rare-earth (4f) systems, the situation is less clear for the actinide (5f) materials. So far the magnetic response has been reported over a limited energy range for only a handful of uranium metallic compounds[1-2]. They show mainly broad excitation spectra similar to those observed in the rare-earth mixed-valent systems. For the magnetic semiconductor, UO_2, the localized nature of the 5f electrons has been studied extensively by optical spectroscopy[3] and neutron diffraction.[4] The crystal-field splitting of the ground-state multiplet, on the other hand, has not heretofore been measured directly. In view of the lack of data from microscopic measurements, especially in the high-energy region (> 100

meV), it is important to direct our experimental efforts to a systematic study of the ground-state level structures and the magnetic response in these interesting materials.

The spin dynamics of itinerant magnetic systems such as iron, nickel and chromium is also not completely understood. In particular, the spin-wave spectra of these metals in the ordered state extend to very high energies at which precise measurements of the magnetic excitations by neutron scattering techniques are difficult at present. Recent theoretical calculations[5] of the dynamic susceptibility of iron and nickel have predicted the existence of optical magnon modes and the disappearance of the spin-waves into the Stoner continuum at high energies. A thorough test of the theory will have to await future experimental investigations.

With the advance of pulsed spallation neutron sources and installation of hot moderators at steady-state reactors, neutron scattering studies of elementary excitations in magnetic materials can now be extended to energies up to about 300 meV. In the present paper we report the recent measurements of magnetic excitations in some d and f transition metals and compounds at the Intense Pulsed Neutron Source (IPNS) of Argonne National Laboratory.

II. Experimental Details

The application of inelastic neutron scattering techniques in the study of magnetic materials has provided a great deal of unique information on the solid-state wave function and the spin dynamics of the systems. However, so far the majority of neutron scattering experiments have been focused on magnetic excitations within or below the thermal energy region (< 80 meV). In order to maximize the scattering probability at larger energy transfer, the principle of detailed balance implies the requirement of using neutrons of high incident

energies so that neutrons lose energy to the system. Moreover, due to the finite extent of the spatial distribution of the electrons contributing to the scattering process, the intensity of magnetic scattering is modulated by the square of the neutron magnetic form factor, $|f(\vec{Q})|^2$, which falls off rapidly as the neutron momentum transfer Q increases. Consequently, kinematic considerations demand the use of even higher incident energies of several times the desired energy transfer in conjunction with rather low scattering angles ($< 10°$).

The spectrum of neutrons emerging from a steady-state reactor shows a Maxwellian distribution roughly in equilibrium at the temperature of the moderator in use. Thus, it covers a rather limited range of energy. A pulsed neutron source, on the other hand, provides neutrons of comparable flux from thermal energy up to the eV range. The spectrum[6] consists of an approximately-Maxwellian distribution in equilibrium at a temperature about 25-50% higher than the physical temperature of the moderator, joined to a "neutron slowing down" component in the epithermal energy region. The ratio of the integrated neutron flux at thermal energy (~ 25 meV) to that at epithermal energy (~ 1 eV) varies typically from three to five.Therefore, a pulsed neutron source is ideally suited for investigations of excitations at high energy transfers. At IPNS, we have measured, using the chopper spectrometers and time-of-flight techniques, the magnetic response functions of a series of d and f transition metals and compounds over a widge range of energy and momentum transfer. The schematic of the Low-Resolution (LRMECS) and High-Resolution (HRMECS) Medium-Energy Chopper Spectrometers is shown in Figure 1. Since the details of the IPNS chopper spectrometers have been given elsewhere,[7] we shall only give a brief description of the operation here. A phased Fermi chopper produces pulses of monochromatic neutrons which are incident on the sample. The energy and momentum transfer are

determined by neutron time-of-flight techniques in over 120 detectors. A variety of choppers have been designed to select neutrons of energies ranging from ~ 30 meV to about 1 eV. The energy resolution in general depends on the chopper in use and varies with energy transfer but is approximately 6-8% of the incident energy for LRMECS and about 3-4% for HRMECS. Measurements of elastic incoherent scattering from a thin plate of vanadium provide detector calibration and intensity normalization.

III. Results and Discussion

A. Crystal-field transition in PrO_2, $BaPrO_3$, UO_2 and CeB_6

The neutron scattering cross section for crystal-field transitions in a system of noninteracting magnetic ions consists of sharp peaks at energies corresponding to the splittings of the levels where transitions occur. The line intensity is proportional to the square of the matrix elements weighted by the Boltzmann factor and the observed line width is that of the instrumental resolution. (Intrinsic width is proportional to the width of the 4f resonance, which is very small.) However, in stoichiometric compounds and especially in metallic systems, inter- and intraionic coupling and screening by conduction electrons may give rise to line broadening and renormalization of scattered intensity. Here one can envisage a series of experiments, on both stoichiometric and non-stoichiometric materials, on the one hand to determine the effects of various anions and configuration interactions, and on the other hand to study the coupling mechanism between the f moments and conduction electrons.

We have concentrated on PrO_2, $BaPrO_3$ and UO_2 for the reason of their simple structures (cubic fluorite structure for the dioxides and perovskite for $BaPrO_3$). A crystal-field of cubic symmetry will split the ionic ground state of the $Pr(4f^1)$ ion ($^2F_{5/2}$) into a Γ_7 doublet and a Γ_8 quartet, and that ($^3H_4$) of $U(5f^2)$

ion into a Γ_5 triplet, Γ_3 doublet, Γ_4 triplet and a Γ_1 singlet. Observation of the crystal-field excitations in these materials by optical techniques such as Raman scattering has been difficult because of the optical opacity of these compounds. Inelastic neutron scattering represents the best known method for direct measurements.

The neutron spectra for PrO_2[8], obtained by using the HRMECS with incident neutron energy of 350 meV, is shown in Figure 2. A peak at 135 ± 5 meV is clearly evident. That the peak is magnetic in origin was established by the rapid decrease in the peak intensity as a function of momentum transfer Q, and by the fact that no peak was observed in a similar experiment on CeO_2. (CeO_2 has no localized 4f electron, therefore no peak is expected.) The assignment of the transition as between the Γ_8 ground state and the Γ_7 excited state is consistent with the analysis of magnetic susceptibility data.[9] Furthermore, since the observed line width (FWHM = 15 meV) is larger than the instrumental resolution (~10 meV), the authors[8] proposed the possibility of a dynamic Jahn-Teller[10] effect in PrO_2. Such an effect will lift the degeneracy of the Γ_8 quartet via a quadrupole interaction and lead to an explanation for moment reduction[11] in the ordered state.

The neutron scattering experiment on $BaPrO_3$[12] represents an interesting extension of the PrO_2 measurements. The Pr ion in $BaPrO_3$ is surrounded by six oxygen nearest neighbors in an octahedral array rather than by eight oxygen neighbors forming a cube as in PrO_2 (see Figures 2 and 3). By scaling the results in PrO_2 based on geometric and symmetry considerations one would expect a Γ_7 doublet ground state and a splitting about 240 meV between the Γ_7 and Γ_8 states in $BaPrO_3$. In a search for the crystal-field excitation in $BaPrO_3$ we have performed neutron scattering experiments on HRMECS using incident energies of 500

and 800 meV. In both runs a sharp peak at 259 ± 2 meV was clearly identified (see Figure 3 for the 800 meV run). By examination of the Q dependence of the peak intensity we inferred the magnetic origin of this excitation and therefore suggest a crystal-field splitting of 259 ± 2 meV between the Γ_7 ground state and Γ_8 excited state in $BaPrO_2$. It is also interesting to note that the measured line width of the crystal-field transition in $BaPrO_3$ is resolution limited, as contrasted with the broadened intrinsic width observed in PrO_2.

Our recent experiments on UO_2 were the first step in extending the investigations of crystal field level structures to the 5f system. UO_2 exhibits a first-order antiferromagnetic transition[3] (so does PrO_2) at T_N = 30.8K with an ordered moment[4] of 1.74μ_B/f.u. at 4.2K, a value smaller than the moment of 2μ_B for the Γ_5 ground state of the $^3H_4$ ($5f^2$) state. A neutron diffraction study[4] showed that there is an internal distortion of the lattice due to oxygen displacements in the ordered state. The present inelastic neutron experiments in UO_2 consisted of measurements of the excitation spectra at 10, 27, 48K with neutron incident energy E_0 = 350 meV, at 45K with E_0 = 500 meV and at 296K with E_0 = 800 meV. A similar run at E_0 = 500 meV on the nonmagnetic isostructural compound ThO_2 served as a reference for phonon scattering and background. The excitation spectra of UO_2 with E_0 of 350 meV are shown in Figure 4.

Preliminary data analysis indicated that the major peak at 156 meV (see Figure 4) corresponds to the crystal-field excitation from the Γ_5 ground state to the Γ_3 excited state. This value is in good agreement with that (~ 170 meV) first estimated by Rahman and Runciman.[13] The origin of the second peak at about 172 meV is presently not understood. One possibility is that the degeneracy of the Γ_3 doublet is lifted by a quadrupole interaction and the two peak structure

represents the crystal field transitions from the ground state to these two levels.

The above experiments also provided a unique opportunity for a direct comparison of the measured $A_4 \langle r^4 \rangle$ terms in the crystal-field potential of PrO_2 and UO_2, from which we hope to obtain physical insight into the importance of J-mixing effects in the 5f materials. This subject is of considerable interest because it may lead to a better understanding of the classification scheme for angular momentum coupling in 5f systems. Detailed analysis of the above results will be presented[12] elsewhere.

Finally we shall briefly discuss the crystal-field splitting in an intermetallic compound CeB_6. The determination of the magnetic ground state level structure is crucial for the interpretation of the observed Kondo effect[14] and large reduction of the Ce moment[15] in the ordered state in this material. Unfortunately a serious discrepancy exists between results[15] obtained from a variety of investigations. An earlier inelastic neutron scattering experiment[15] in the thermal energy range precluded the existence of the Γ_7-Γ_8 crystal-field transition up to about 40 meV. Naturally this led to a search for the crystal-field transition at higher energies. In the recent measurement[16] at IPNS we find that the Γ_7-Γ_8 crystal-field excitation occurs at 47 ± 1 meV (see Figure 5). We have also initiated a systematic study of the temperature dependence of the line width and peak intensity in order to assess the importance of interaction between the 4f moments and conduction electrons in this compound. The results of these measurements will be published[17] separately.

B. Magnetic excitations in the mixed-valent alloy $Ce_{.74}Th_{.26}$

In this section, we briefly describe a recent study[18] of the paramagnetic response functions of the mixed-valent alloy $Ce_{.74}Th_{.26}$. The physical properties

of the alloy system $Ce_{1-x}Th_x$, in particular those related to valence instability and spin fluctuations of the f electrons, have been studied[19,20] extensively. In the present sample (x = 0.26) a first-order phase transition[19] corresponding to the cerium $\gamma \leftrightarrow \alpha$ phase change in the alloy occurs at about 150K. Results of earlier work[19] using thermal neutrons revealed a broad magnetic spectral response with significant intensity extending to the energies beyond the limit of those measurements (~ 70 meV). The present experiment aimed at the determination of the magnetic response in this material over a wide range of energy and momentum transfer and temperatures, thereby obtaining a quantitative description of the spin dynamic susceptibility. A reliable extraction of the magnetic scattering from the observed intensity is very important in these measurements. For example, Shapiro and co-workers[19] devoted particular care to the procedures of phonon subtraction in the analysis of the low-energy CeTh data. In the present experiments, we have adopted the method of phonon subtraction and procedures for internal consistency checks given by these authors. We have also improved the shielding in the spectrometers to minimize, as much as possible, the background level.

Figure 6 shows the temperature dependence of the imaginary part of the magnetic susceptibility (as defined in Ref. 19), $\chi''(Q,E)$ for $Ce_{.74}Th_{.26}$ measured at a fixed scattering angle. Two observations should be made. First, since Q increases with the energy transfer (see Figure 7), the decrease of the susceptibility at large energy is partly due to the vanishing form factor in that region. Therefore $\chi''(Q,E)$ for constant Q actually extends to even higher energies. Second, the abrupt change in the shape and magnitude of the magnetic susceptibility between temperatures above and below the transition is connected to the nature of the first-order phase transition[19] in the alloy of this Ce

concentration. In general, it was found that the width of χ'' varies as the inverse of the static susceptibility.

Since rigorous calculation of the dynamic susceptibility for mixed-valent materials is presently unavailable, we resorted, as previously,[19,20] to fitting the data by a spectral function corresponding to a purely relaxational system, namely,

$$\chi''(Q,E) \sim |f(Q)|^2 \, E \, \frac{\gamma}{E^2 + \gamma^2} \quad . \tag{1}$$

The magnetic form factor[21] of Ce^{3+} free ion was used in the least-squares analysis. We find that the width, γ, changes from about 17 meV in the γ-phase to about 160 meV in the α-phase. The large value of γ in the α-phase could not be estimated accurately in the previous experiment[19] because it exceeds the energy range of that measurement. The width γ provides a measure of the spin-fluctuation energy. The present results therefore indicate that in the γ-phase, the spin-fluctuation energy $h\gamma$ is comparable with the thermal energy kT, whereas in the α-phase, the spin-fluctuation energy is much greater than the thermal energy. Instead it is more comparable with the f bandwidth[22] resulting from hybridization of 4f and conduction-band states. Within experimental precision, the present data show no evidence of additional inelastic peaks other than the quasielastic component. However, inelastic features may exist in other mixed-valent materials. Furthermore, the assumption of a purely relaxational spin dynamics for mixed-valent systems is not easy to justify physically. Therefore, it is hoped that more measurements of the paramagnetic response in the high energy region in other mixed-valent materials will lead to a more realistic expression.

C. Spin-wave spectrum of ferromagnetic iron at low temperature

Complete measurements of the magnon dispersion relation of iron by neutron scattering are difficult because the excitation spectrum extends to very high energies. Collins et al.[23] made high resolution measurements of the magnons in iron up to energies of ~ 70 meV and found that the excitation spectrum was completely isotropic in reduced wave vector $\vec{q}$ over this range. Mook and Nicklow[24] extended these measurements in the [110] direction to about 110 meV in pure iron, while in a large crystal of ^{54}Fe(4%Si) they found a dramatic decrease in spin-wave intensities for $E \gtrsim 90$ meV. Lynn[25] found a similar decrease in spin-wave intensities in a sample of ^{54}Fe(12%Si) for $E \gtrsim 120$ meV.

In a recent experiment[26] using a single crystal sample we have extended the spin-wave measurements in pure iron at 10K up to energy transfer of about 160 meV. The spin-waves over the entire range of energy are found to be consistent with an isotropic spin-wave dispersion relation (see Figure 7). We find that the observed spin-wave intensity in the energy range of 40-160 meV monotonically decreases with increasing energy. Such an energy dependence of the spin-wave intensity is expected from band structure effects in itinerant ferromagnets. Recent theory[5] predicted that the existence of an "optical" magnon mode at higher energies, with scattering strength considerably smaller than that of the "acoustic" spin wave at low energies. With the present experimental sensitivity we were unable to observe any additional magnetic excitations.

IV. Conclusion

We have briefly described some results of recent neutron scattering experiments at IPNS in the studies of magnetic excitations at high energy transfers. Specifically, we have observed crystal-field excitations in some rare-earth and actinide compounds in energy range from 40 to 260 meV and we also

extended the measurements of the paramagnetic response in a mixed-valent alloy, $Ce_{.74}Th_{.26}$, to energy of about 250 meV. The significance of the neutron scattering results in relation to ground state level structures of the magnetic ions and the spin dynamics of the f electrons are discussed. Accurate determination of spin-wave intensities and Stoner excitations in itinerant magnets at high energy is still difficult. However, we should point out that inelastic neutron scattering investigation of magnetic systems at energies beyond the thermal region is still in its infancy. With further development in instrumental sensitivity and neutron source intensity in the near future, we look forward to exciting new opportunities in the field of high energy magnetic spectroscopy.

Acknowledgements

The author is indebted to the many collaborators with whom he has enjoyed working in the course of these studies. They are J. M. Carpenter, J. Faber, B. H. Grier, S. Kern, G. H. Lander, J. M. Lawrence, M. Loewenhaupt, J. W. Lynn, H. A. Mook, R. A. Robinson, S. M. Shapiro, and S. K. Sinha. In addition, the author wishes to thank all his colleagues and the technical staffs in the MST and IPNS Divisions, ANL; without their support and assistance, the experiments would have been impossible.

References

1. W. J. L Buyers, A. F. Murray, J. A. Jackman, T. M. Holden, P. de V. Duplessis and O. Vogt, J. Appl. Phys. 52, 2222 (1981).
2. M. Loewenhaupt, G. H. Lander, A. P. Murani and A. Murasik, J. Phys. C 15, 6199 (1982).
3. J. Schoeres, Phys. Rep. 63, 301 (1980) and references therein.
4. J. Faber, Jr. and G. H. Lander, Phys. Rev. B 14, 1151 (1976).
5. J. F. Cooke, J. W. Lynn and H. L. Davis, Phys. Rev. B 21, 4118 (1980).
6. J. M. Carpenter, Nucl. Inst. Methods 145, 91 (1977).
7. D. L. Price, J. M. Carpenter, C. A. Pelizzari, S. K. Sinha, I. Bresof, and G. E. Ostrowski, Proceedings of the Sixth Meeting of the International Collaboration on Advanced Neutron Sources, June 28-July 2, 1982, ANL 82-80 (1983), p. 207.
8. S. Kern, C.-K. Loong, J. Faber, Jr. and G. H. Lander, Solid State Comm. 49, 295 (1984).
9. A. B. Tveten and S. Kern (to be published).
10. K. Sasaki and Y. Obata, J. Phys. Soc. Japan 28, 1157 (1970).
11. S. Kern, J. Chem. Phys. 40, 208 (1964).
12. S. Kern, J. Faber, Jr., G. H. Lander and C.-K. Loong (to be published).
13. H. U. Rahman and W. A. Runciman, J. Phys. Chem. Solids 27, 1833 (1966).
14. K. Winzer and W. Felsch, J. Phys. Paris 39, Colloq. 6-832 (1978).
15. S. Horn, F. Steglich, M. Loewenhaupt, H. Scheuer, W. Felsch and K. Winzer, Z. Phys. B 42, 125 (1981) and references therein. See also G. Schell, H. Winter, H. Rietschel and F. Gompf, Phys. Rev. B 25, 1589 (1982).
16. E. Zirngiebl, B. Hillebrands, S. Blumenröder, G. Güntherodt, M. Loewenhaupt, J. M. Carpenter, K. Winzer and Z. Fisk, Phys. Rev. B 30, 4052 (1984).
17. M. Loewenhaupt, J. M. Carpenter and C.-K. Loong (to be published).

18. S. M. Shapiro, B. H. Grier, S. K. Sinha, R. D. Parks, J. M. Lawrence and C.-K. Loong (to be published).

19. S. M. Shapiro, J. D. Axe, R. J. Birgeneau, J. M. Lawrence and R. D. Parks, Phys. Rev. B 16, 2225 (1977).

20. B. H. Grier, R. D. Parks, S. M. Shapairo and C. F. Majkrzak, Phys. Rev. B 24, 6242 (1981) and references therein.

21. C. Stassis, W. H. Deckman, B. N. Harmon, J. D. Desclaux and A. J. Freeman, Phys. Rev. B 15, 369 (1977).

22. S. H. Liu and K.-M. Ho, Phys. Rev. B 28, 4220 (1983).

23. M. F. Collins, V. J. Minkiewicz, R. Nathans, L. Passell and G. Shirane, Phys. Rev. 179, 417 (1969). See also G. Shirane, V. J. Minkiewicz and R. Nathans, J. Appl. Phys. 39, 383 (1968).

24. H. A. Mook and R. M. Nicklow, Phys. Rev. B 7, 336 1973).

25. J. W. Lynn, Phys. Rev. B 11, 2624 (1975).

26. C.-K. Loong, J. M. Carpenter, J. W. Lynn, R. A. Robinson and H. A. Mook, J. Appl. Phys. 55, 1895 (1984).

Figure Captions

Figure 1 Schematic of Chopper Spectrometers at the Intense Pulsed Neutron Source, ANL

Figure 2 Neutron intensity as a function of energy transfer for PrO_2 as observed by detectors with scattering angles less than 7 degrees. Upper left insert: the cubic fluorite structure of PrO_2, the solid and open circles represent, respectively, the Pr and O atoms. Upper right insert: schematic of the $\Gamma_8 - \Gamma_7$ splitting of the J = 5/2 multiplet. The degeneracy of the Γ_8 ground state is lifted by a dynamic Jahn-Teller effect, and, in the ordered state, by the exchange field. The neutron excitation corresponds to the total cross section between all states Γ_8 to both Γ_7 doublet states.

Figure 3 The measured scattering function S(E) of $BaPrO_3$ using the HRMECS with incident energy of 800 meV. Insert: the Pervoskite crystal structure of $BaPrO_3$. Open circles - oxygen; solid circle - praseodymium; and shaded circles - barium atoms.

Figure 4 Energy excitation spectrum of UO_2 at 10, 27, and 48K. Solid curves were obtained by fitting Gaussian functions to the data. The peaks at about 156 meV correspond to the crystal-field excitation from the Γ_5 ground state to the Γ_3 excited state (see text).

Figure 5 Measured S(Q,E) of CeB_6 by the LRMECS with incident neutron energy of 185 meV at two scattering angles, ϕ. (a) At $\phi = 9°$ ($2 < Q < 4\text{Å}^{-1}$), a peak at 47 meV corresponding to the crystal-field transition between the Γ_7 and Γ_8 states, is clearly evident. (b) At $\phi = 100°$ ($9 < Q < 16\text{Å}^{-1}$), the crystal-field excitation at 47 meV can no longer be observed because the form factor in this Q range is exceedingly small. Instead S provides a measure of the effective phonon density of states. (Phonon intensity generally increases as Q^2.) For example, the peak at about 85 meV can be identified as the T_{2g} vibrational mode observed in Raman scattering.[15]

Figure 6 Temperature dependence of the observed imaginary part of the magnetic susceptibility for $Ce_{.74}Th_{.26}$. The solid curves show the results of fitting the spectral function given in Eq. (1) to the experimental data. The widths, γ, obtained are 17.4 ± 0.7, 25.3 ± 1.3, 87.4 ± 9.4 and 159.5 ± 26 meV respectively for the spectra at 200, 155, 140 and 100K.

Figure 7 Spin-wave spectrum of pure iron at 10K. Incident neutron energies of 200, 300 and 350 meV have been used to measure the magnetic excitations from 40 to 160 meV. The solid curve shows the results of fitting the dispersion relation, $E = D|\vec{q}|^2(1 - \beta|\vec{q}|^2)$, to the experimental data in which D and β were found to be approximately 307 and 0.32 meVÅ^2. The dashed curve is calculated from the above dispersion relation using $D = 325$ meVÅ^2 and $\beta = 0.9$ meVÅ^2.

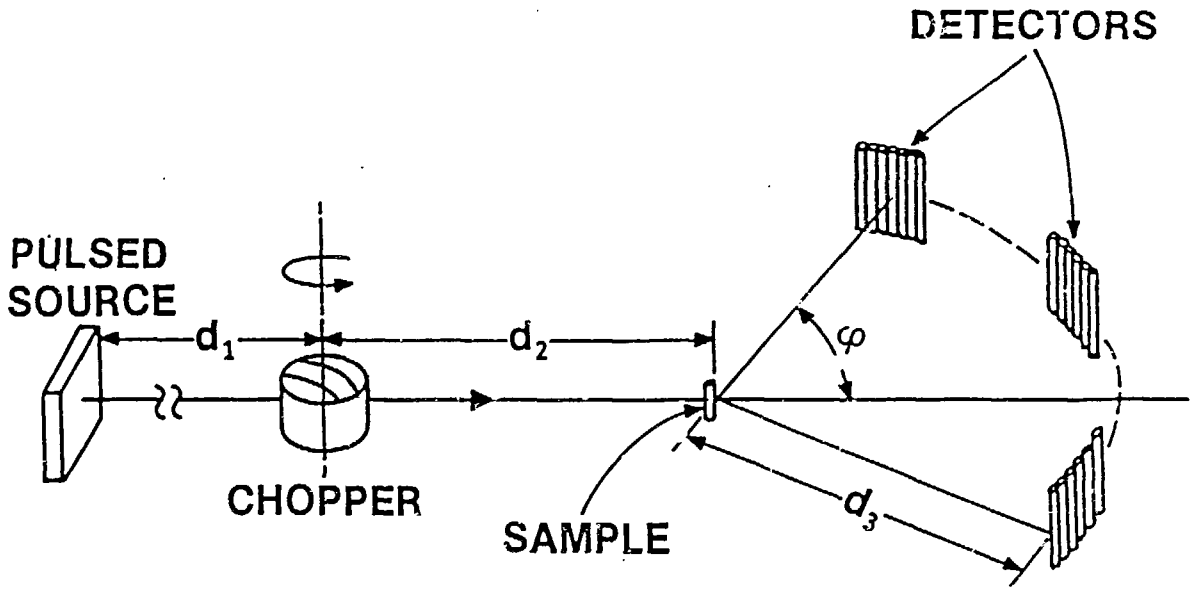

	d_1	d_2	d_3	$\Delta E/E_0$	φ
HRMECS	12.8 m	1.1 m	4.0 m	3-4%	−20° TO +20°
LRMECS	6.1 m	0.7 m	2.5 m	6-8%	-10° TO +120°

Figure 1 Schematic of Chopper Spectrometers at the Intense Pulsed Neutron Source, ANL

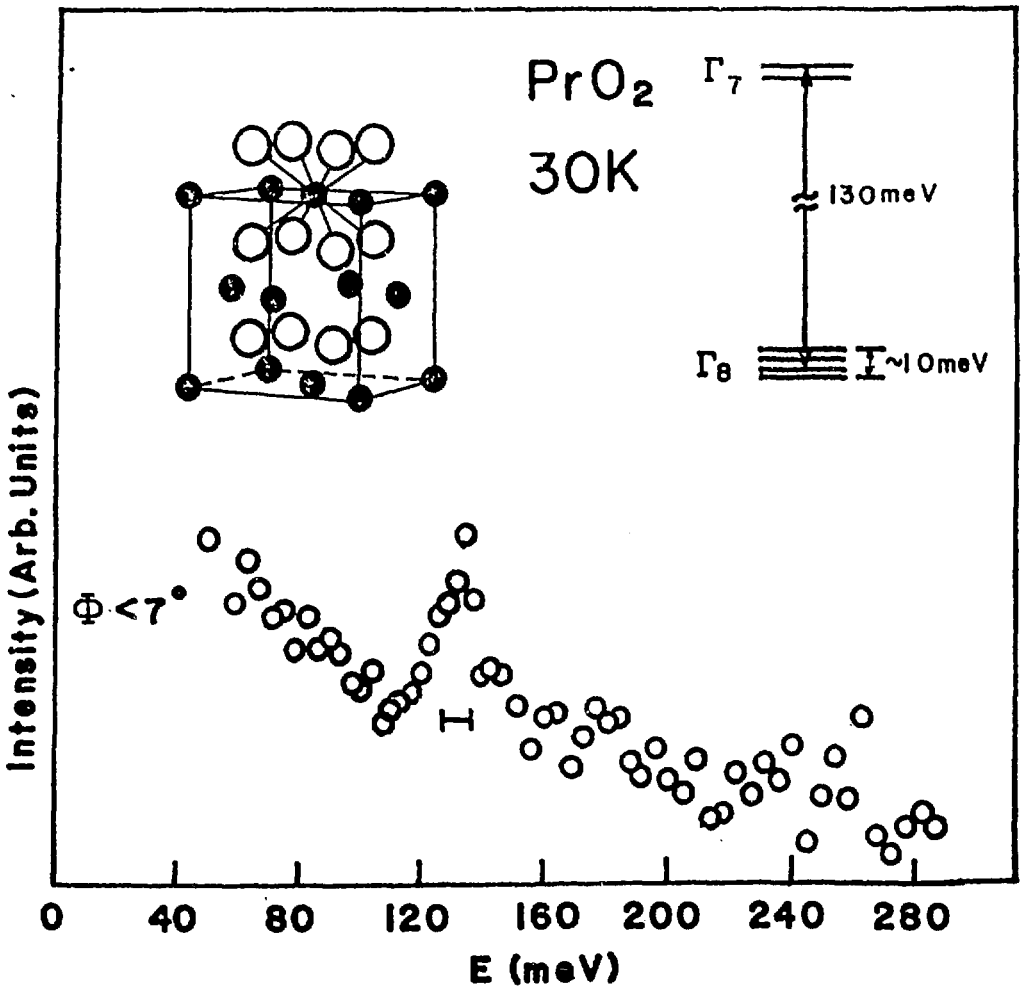

Figure 2 Neutron intensity as a function of energy transfer for PrO_2 as observed by detectors with scattering angles less than 7 degrees. Upper left insert: the cubic fluorite structure of PrO_2, the solid and open circles represent, respectively, the Pr and O atoms. Upper right insert: schematic of the Γ_8 - Γ_7 splitting of the J = 5/2 multiplet. The degeneracy of the Γ_8 ground state is lifted by a dynamic Jahn-Teller effect, and, in the ordered state, by the exchange field. The neutron excitation corresponds to the total cross section between all states Γ_8 to both Γ_7 doublet states.

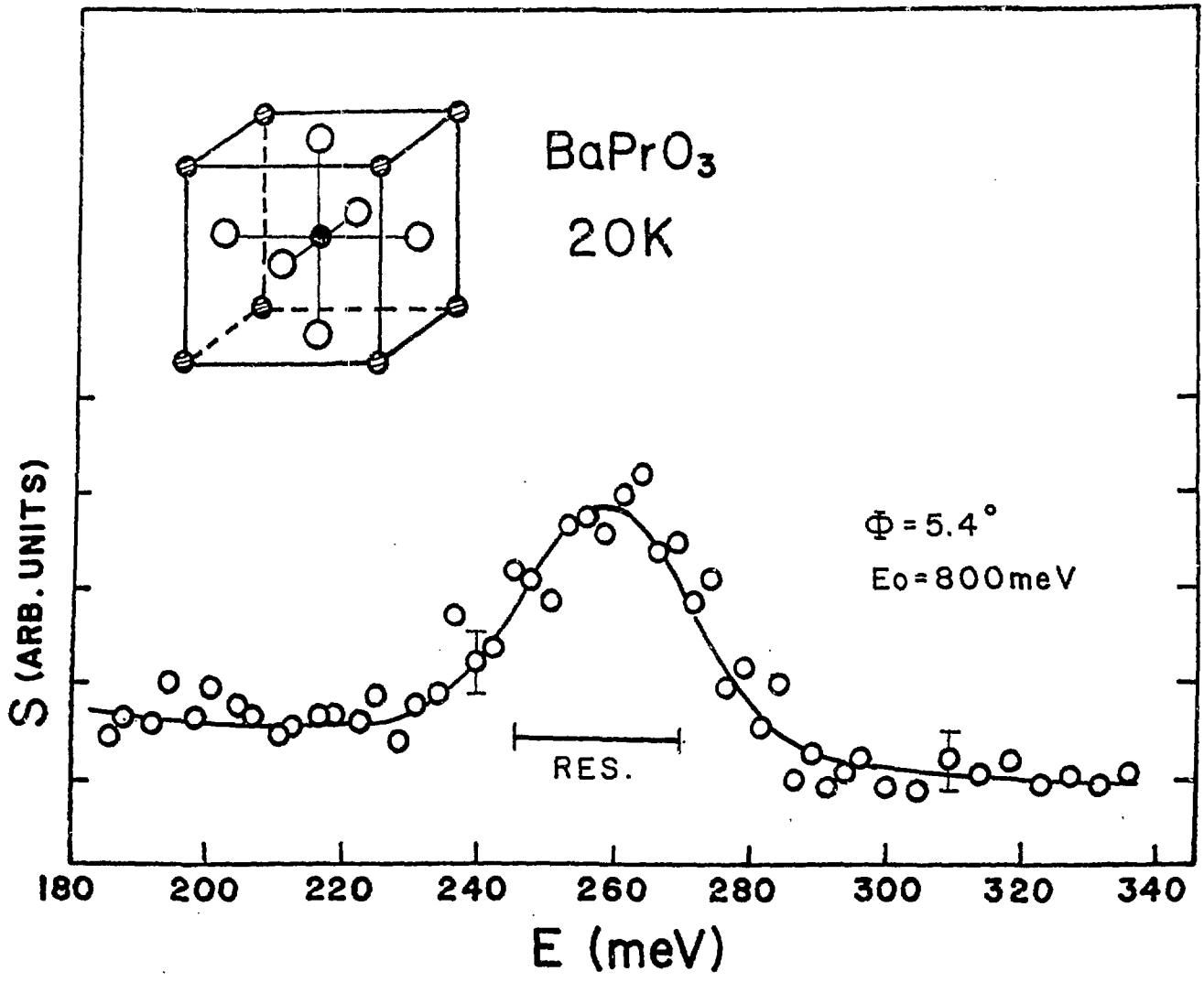

Figure 3 The measured scattering function S(E) of $BaPrO_3$ using the HRMECS with incident energy of 800 meV. Insert: the Pervoskite crystal structure of $BaPrO_3$. Open circles - oxygen; solid circle - praseodymium; and shaded circles - barium atoms.

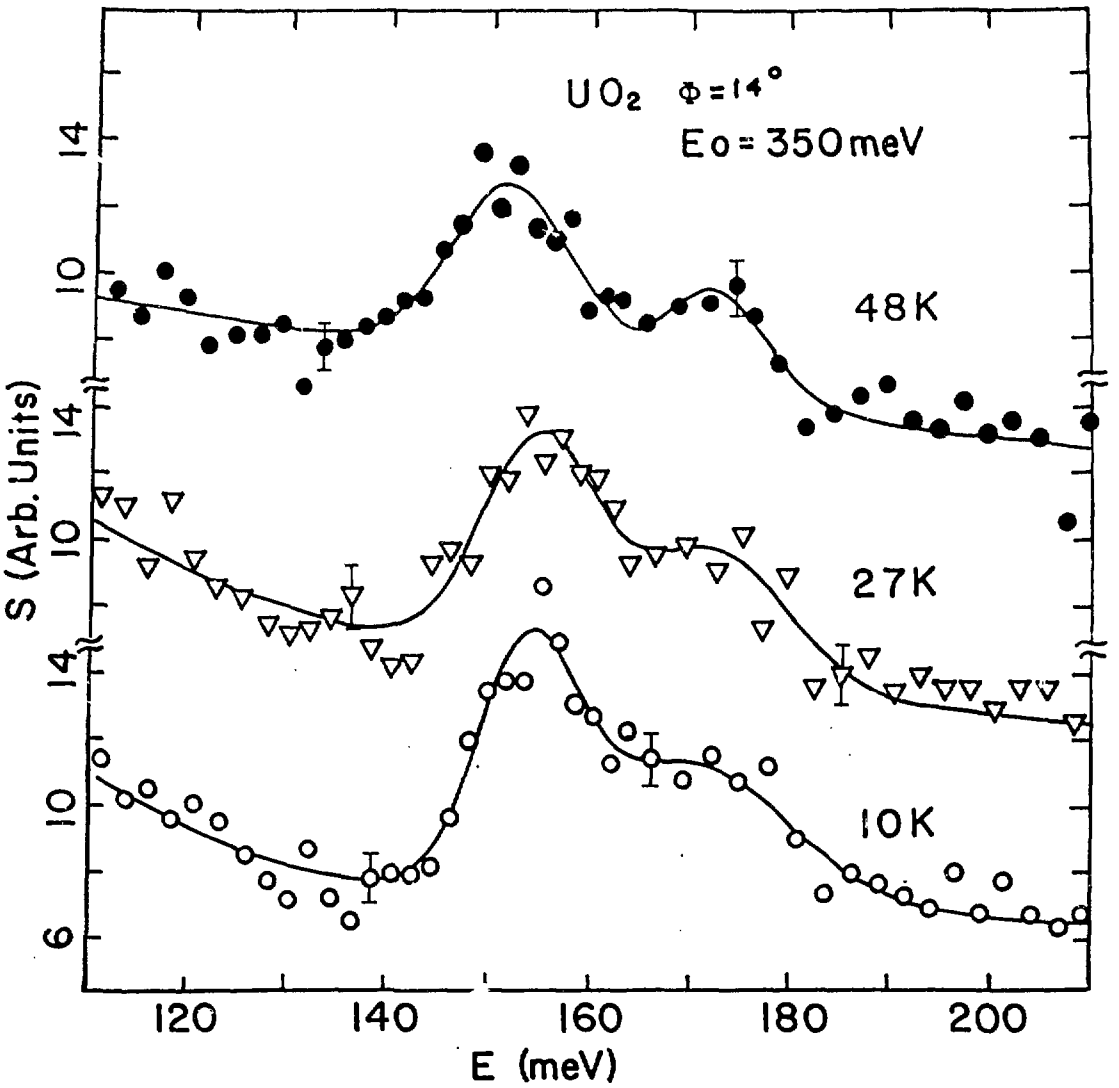

Figure 4 Energy excitation spectrum of UO_2 at 10, 27, and 48K. Solid curves were obtained by fitting Gaussian functions to the data. The peaks at about 156 meV correspond to the crystal-field excitation from the Γ_5 ground state to the Γ_3 excited state (see text).

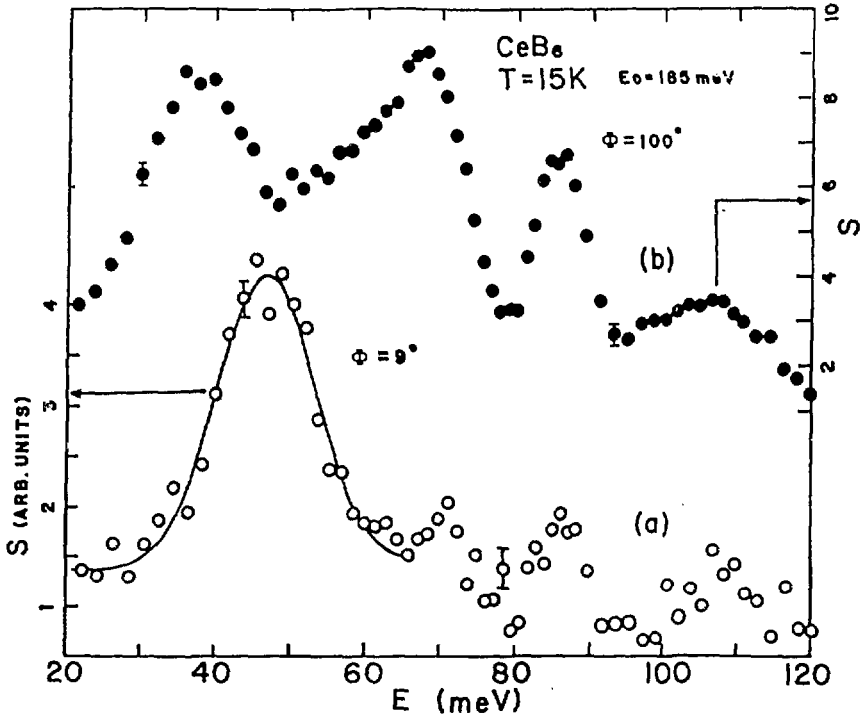

Figure 5 Measured $S(Q,E)$ of CeB_6 by the LRMECS with incident neutron energy of 185 meV at two scattering angles, ϕ. (a) At $\phi = 9°$ ($2 < Q < 4\text{Å}^{-1}$), a peak at 47 meV corresponding to the crystal-field transition between the Γ_7 and Γ_8 states, is clearly evident. (b) At $\phi = 100°$ ($9 < Q < 16\text{Å}^{-1}$), the crystal-field excitation at 47 meV can no longer be observed because the form factor in this Q range is exceedingly small. Instead S provides a measure of the effective phonon density of states. (Phonon intensity generally increases as Q^2.) For example, the peak at about 85 meV can be identified as the Γ_{2g} vibrational mode observed in Raman scattering.[15]

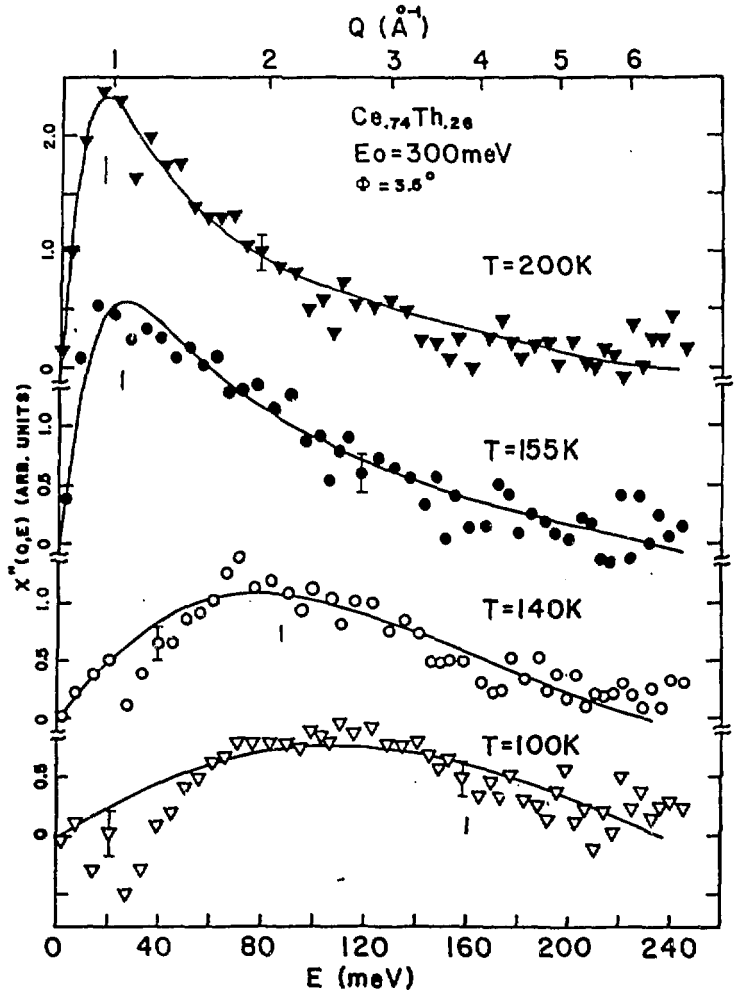

Figure 6 Temperature dependence of the observed imaginary part of the magnetic susceptibility for $Ce_{.74}Th_{.26}$. The solid curves show the results of fitting the spectral function given in Eq. (1) to the experimental data. The widths, γ, obtained are 17.4 ± 0.7, 25.3 ± 1.3, 87.4 ± 9.4 and 159.5 ± 26 respectively for the spectra at 200, 155, 140 and 100K.

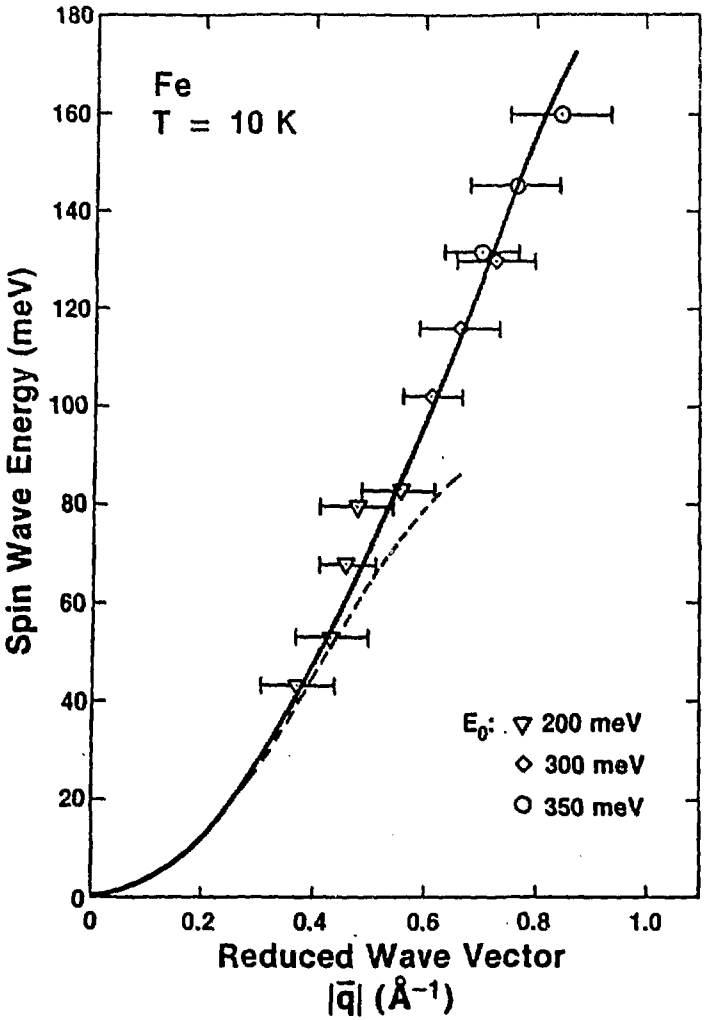

Figure 7 Spin-wave spectrum of pure iron at 10K. Incident neutron energies of 200, 300 and 350 meV have been used to measure the magnetic excitations from 40 to 160 meV. The solid curve shows the results of fitting the dispersion relation, $E = D|\vec{q}|^2(1 - \beta|\vec{q}|^2)$, to the experimental data in which D and β were found to be approximately 307 and 0.32 meVÅ^2. The dashed curve is calculated from the above dispersion relation using D = 325 meVÅ^2 and β = 0.9 meVÅ^2.